ISCI, Volume *23*

Supplemental Information

Thermoelectric Flexible Silver Selenide Films: Compositional and Length Optimization

Jie Gao, Lei Miao, Huajun Lai, Sijing Zhu, Ying Peng, Xiaoyang Wang, Kunihito Koumoto, and Huanfu Cai

Supplemental Information

This PDF file includes:

Transparent Methods

Figure S1 to S7

Table S1

Video S1

Transparent Methods

EXPERIMENTAL PROCEDURES

Materials

Silver nitrate ($AgNO_3$, 99.8%) , selenium powder (Se, 99.9%), ethylenediamine ($C_2H_8N_2$, 99%) and polyvinylpyrrolidone (PVP, M.W. 58000) were purchased from Aladdin Chemical Co., Ltd. Ethylene glycol ($C_2H_6O_2$, 99%) was bought from Sinopharm Chemical Reagent Co., Ltd. The glass fiber membrane was obtained from Yuyan (Shanghai) Chemical Co. and the copy-paper was produced by Onhing (Shanghai) Paper Co., Ltd. All of these materials were used without further purification.

Preparation of silver selenide NPs dispersion

First, a certain amount of Se powder and 10 mg PVP were dissolved in 15 mL ethylenediamine under vigorous magnetic stirring at room temperature for 30 min. Then, under ultra-sonication, some $AgNO_3$ was dissolved in 5 mL ethylenediamine at room temperature. Subsequently, the $AgNO_3$ solution was quickly poured in the Se solution and the mixture was transferred into a 25 mL Teflon-lined stainless steel autoclave. The autoclave was sealed and maintained at 180 ^oC for 5 h. After the autoclave was cooled to room temperature naturally, black precipitate was collected by centrifugation and washed with ethanol for two times. Finally, the product was dispersed in 10 mL of ethylene glycol to form a uniform black dispersion. The total amount of the $AgNO_3$ and Se powder for all samples is 0.4187 g and molar ratio of $AgNO_3$ and Se varies from 1.9 to 2.5.

Fabrication of paper-supporting silver selenide NPs films

First, with the aid of vacuum filtration, 12 drops (the volume of 28 drops is about 1 mL) of silver selenide NPs dispersion were drop-cast on a piece of glass-fiber sheet with size of 20 mm × 5 mm. Then after the glass-fiber sheet coated with silver selenide NPs was dried in dynamic vacuum at 80 ^{o}C for 4 h, it was sandwiched between 2 pieces of copy-paper and pressed at 40 MPa for 30 s. Afterwards the debris of glass-fiber was removed and the paper-supporting silver selenide NPs film was obtained. Finally, in the flowing Ar/H_2 atmosphere, the paper-supporting films were annealed in a tube furnace at 250 ^{o}C for 2 h. The samples were named as $Ag_{1.9}Se$, $Ag_{2.0}Se$, $Ag_{2.1}Se$, $Ag_{2.2}Se$ $Ag_{2.3}Se$, $Ag_{2.4}Se$ and $Ag_{2.5}Se$, however, it should be noted that the actual molar ratios of Ag/Se in the samples do not equal to the corresponding molar ratios of $AgNO_3$ to Se powder.

Characterization

The crystallographic structure of silver selenide films were studied by X-ray diffractometer (XRD) using Cu Ka radiation (Bruker, D8 Advance). The size and morphology of silver selenide nanoparticles and films were revealed by scanning electron microscopy (SEM), operated on a Hitachi S-4800 FESEM microscope and transmission electron microscopy (TEM), performed on a Thermo Fisher Talos F200X microscope. The composition of silver selenide films were analyzed by energy-dispersive X-ray spectroscopy (EDS) using the Oxford energy dispersive X-ray detectors attached with the microscopes. Electrical conductivities and Seebeck coefficients of silver selenide films were taken via a Seebeck coeffcient/electrical resistivity measuring system (Ulvac-Riko, ZEM-3) in argon (99.999%) atmosphere

with temperature gradients of 20, 30 and 40 ^{o}C. Charge carrier mobility and carrier concentration of silver selenide films were obtained by measuring the Hall effect (Toyo, Resitest 8300). The thermal diffusivity was measured via a laser flash diffusivity apparatus (NETZSCH LFA 467). The specific heat capacity was obtained using a differential scanning calorimeter (NETZSCH 404 F3). The resistances of silver selenide films and generators were measured by a multimeter (Fluke, 12E+). Output voltages of paper-supporting generators were collected by a nanovoltmeter (Keithley, 2182A).

Numerical simulation

By finite element modeling, the optimal length of single annealed $Ag_{2.3}Se$ film is numerically simulated through COMSOL Multiphysics 5.4a software. The size of $Ag_{2.3}Se$ film is set as L mm × 5 mm × 10 μm (L is variable), the electrodes are set as 0.5 mm × 5 mm × 10 μm and the paper substrate is set as (L+1) mm × 5mm × 30 μm. The size of aluminum plates is set as 7 mm × 3 mm × 1 mm and the hot side and cold side of aluminum plates are set as 50 ^{o}C and 25 ^{o}C (environmental temperature), respectively. The size of air domain is set as 12 mm × (L+2) mm × 4mm. In the whole model, at the interfaces among the annealed $Ag_{2.3}Se$ film, electrodes, paper substrate and aluminum plates, the contact thermal and electrical resistance are ignored. The thermal conductivities of paper-substrate and annealed $Ag_{2.3}Se$ film are set as 0.8 W/(mK) and 1.8 W/(mK), respectively, and the heat is dissipated from the whole model to atmosphere by natural convection.

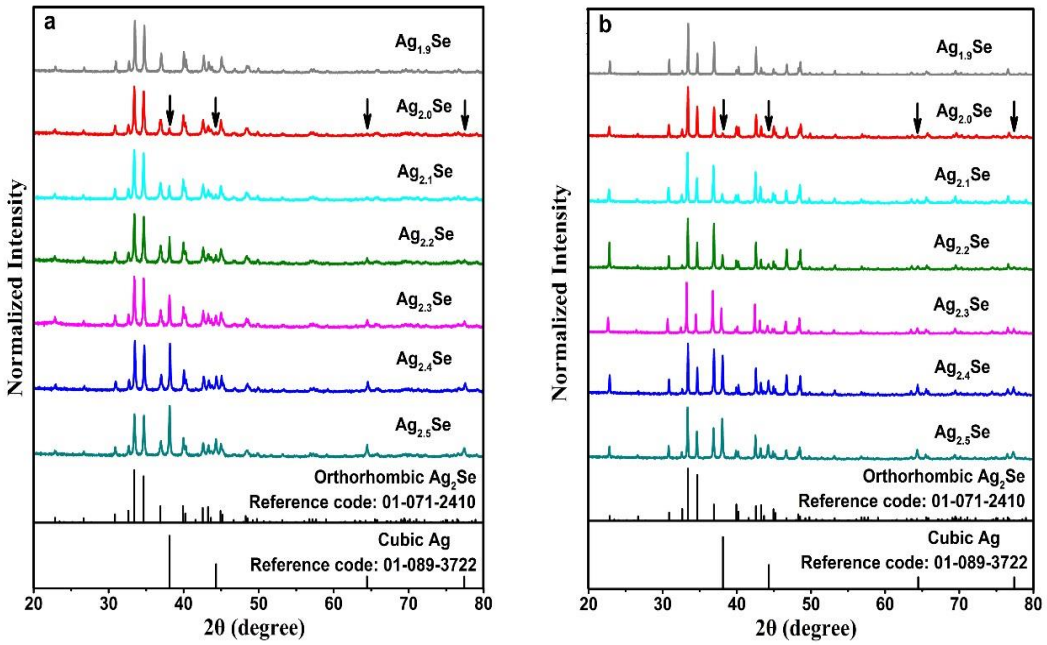

Figure S1. The XRD spectra of all silver selenide films before (a) and after (b) being annealed, related to Figure 1.

As displayed in Figure S1, all peaks in the XRD spectra of $Ag_{1.9}Se$ film can be indexed to the orthorhombic Ag_2Se and the XRD spectra of other films show characteristic peaks of orthorhombic Ag_2Se and cubic Ag. By comparing Figure S1a with Figure S1b, the annealing treatment leads to the weakened intensity of characteristic peaks of Ag and enhanced intensity of some characteristic peaks of Ag_2Se.

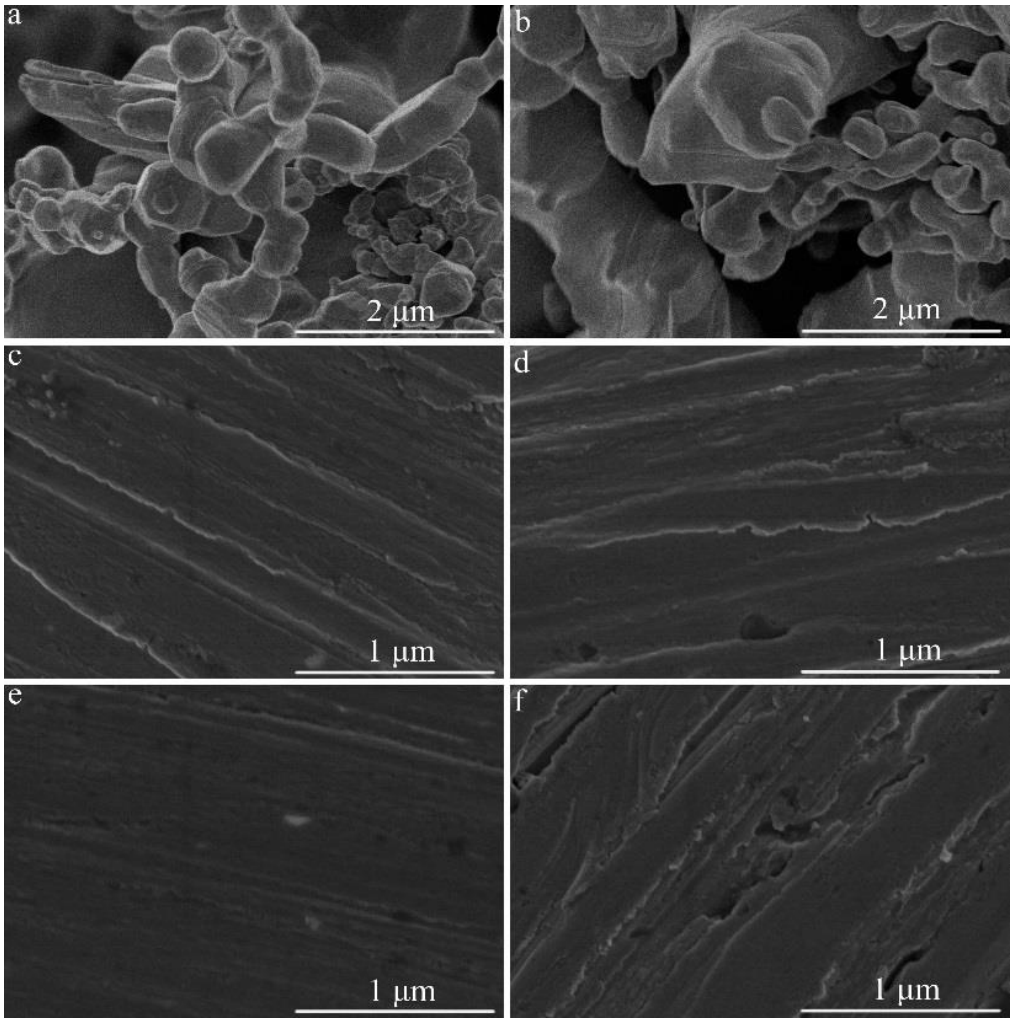

Figure S2. The representative SEM images of silver selenide particles and paper-supporting films. $Ag_{2.1}Se$ and $Ag_{2.3}Se$ particles (a and b), $Ag_{2.1}Se$ and $Ag_{2.3}Se$ films (c and d) and annealed $Ag_{2.1}Se$ and $Ag_{2.3}Se$ films (e and f), related to Figure 3.

Figure S2 reveals the morphology of $Ag_{2.1}Se$ and $Ag_{2.3}Se$ particles and films. As shown in Figure S2a and Figure S2b, the large-sized and small-sized particles with irregular shape can also be found in these two samples. It can be observed from Figure S2c to Figure S2f that the surface morphology of silver selenide films are similar and the annealing treatment has little impact on the morphology of silver selenide films.

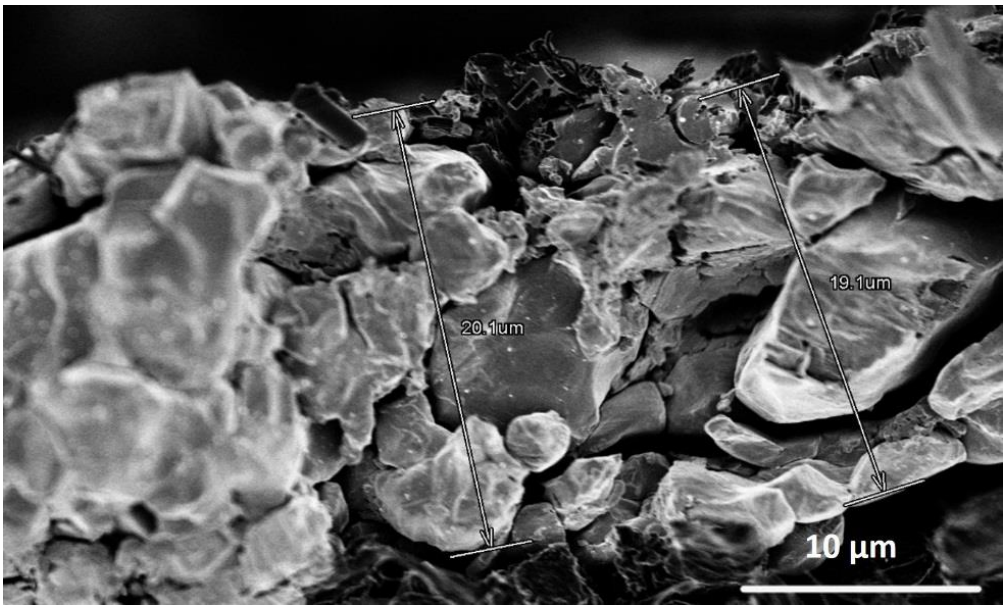

Figure S3. The cross-sectional SEM image of annealed $Ag_{2.5}Se$ film prepared using 25 drops of dispersion, related to Figure 3.

To measure the thickness of the silver selenide film accurately, a piece of annealed $Ag_{2.5}Se$ film is prepared using 25 drops of dispersion, and the cross-sectional SEM image of this film is shown in Figure S3. From this figure, the thickness of this film is about 20 μm, thus the thickness of films prepared with 12 drops of dispersion is about 10 μm.

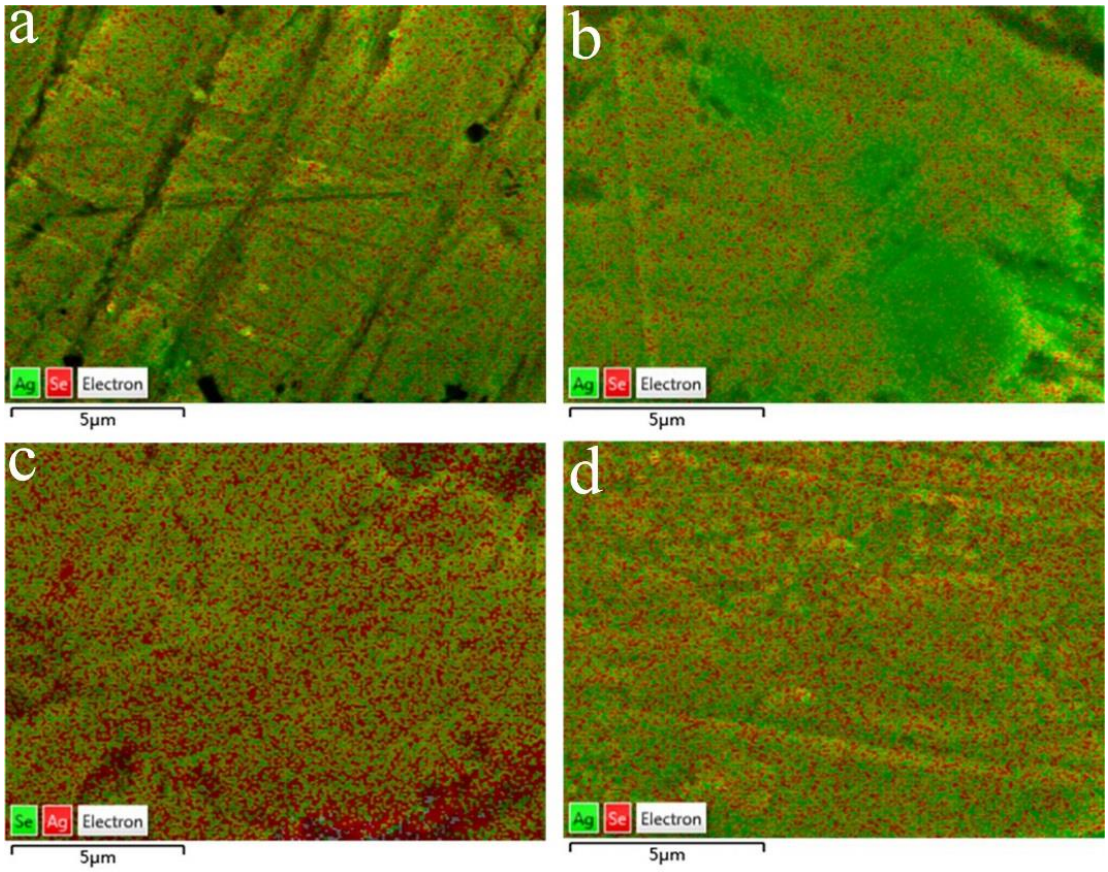

Figure S4. The representative SEM-EDS maps of silver selenide films before and after being annealed. $Ag_{2.1}Se$ film (a), $Ag_{2.3}Se$ film (b), annealed $Ag_{2.1}Se$ film (c) and $Ag_{2.3}Se$ film (d), related to Figure 4 and Table 1.

As shown in Figure S4, compared with the SEM-EDS maps of $Ag_{2.1}Se$ and $Ag_{2.3}Se$ films before being annealed, the signal of Ag element in SEM-EDS maps of corresponding annealed films is obviously reduced and the area of Ag aggregations in annealed $Ag_{2.3}Se$ films is also remarkably diminished.

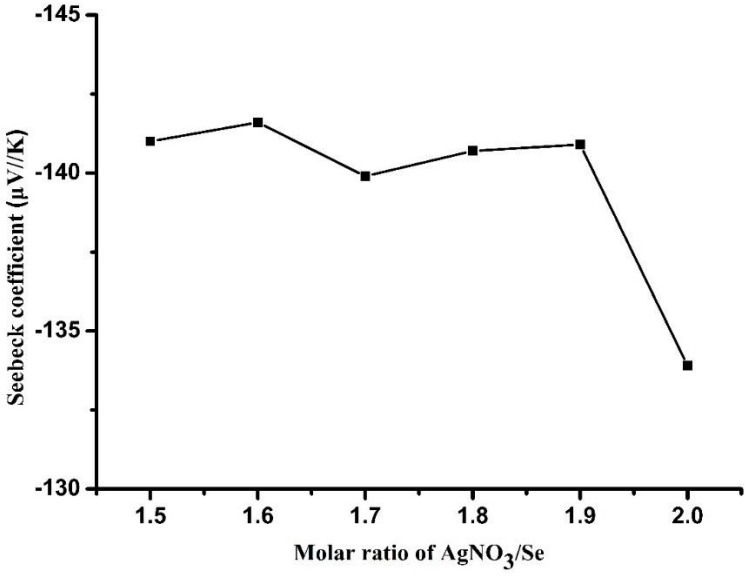

Figure S5. The Seebeck coefficient at 303 K of silver selenide films (from $Ag_{1.5}Se$ to $Ag_{2.0}Se$) before being annealed, related to Figure 6.

The Seebeck coefficients of films prepared with smaller ratios of $AgNO_3$/Se (from 1.8 to 1.5) are displayed in Figure S5. It can be concluded from this figure that the further reduction of $AgNO_3$ is not helpful to improve the Seebeck coefficient of silver selenide film.

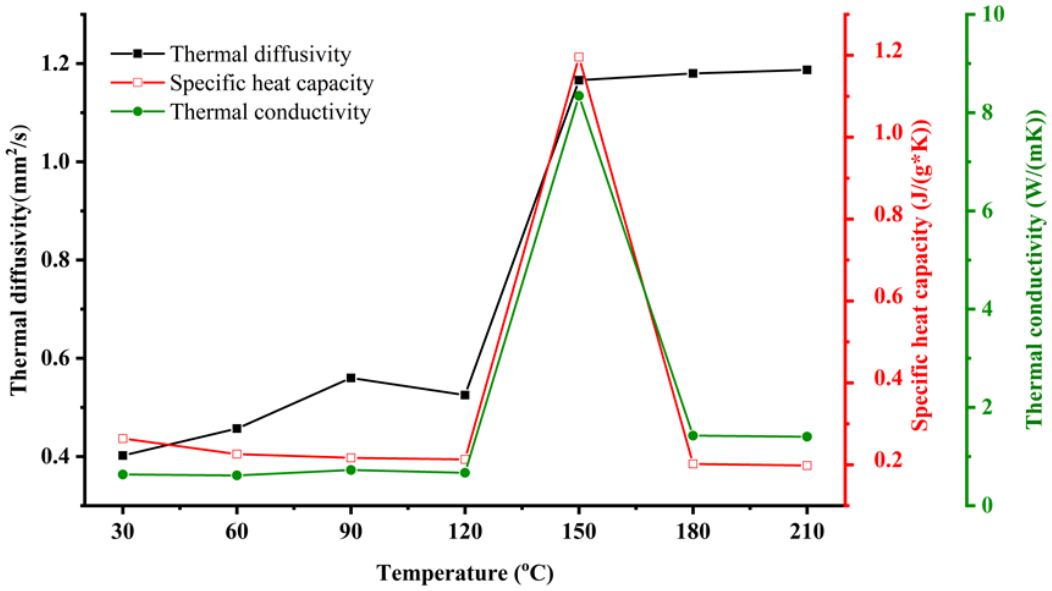

Figure S6. The temperature dependent thermal diffusivity, specific heat capacity and thermal conductivity of annealed $Ag_{2.3}Se$ pellet, related to Figure 8.

In this figure, the thermal conductivity κ is calculated as $\kappa = \alpha * C_p * \rho$, where α is thermal diffusivity, C_p is specific heat capacity and ρ is density of pellet (5.981 g/cm3). As shown in this figure, the thermal conductivity of annealed $Ag_{2.3}Se$ sample at 30 °C is 0.635 W/(mK), and if the ZT value was calculated using this thermal conductivity and PF value of annealed $Ag_{2.3}Se$ film, an ultra-high ZT of 1.12 at 30°C would be obtained. We think that this thermal conductivity is credible but it probably cannot be applied for annealed $Ag_{2.3}Se$ film since the electrical property and thermal conductivity of pellet and film seem to be different due to the influence of substrate. Thus, the theoretic thermal conductivity of silver-rich silver selenide at room temperature of 1.8 W/K is used as the thermal conductivity for our annealed $Ag_{2.3}Se$ film

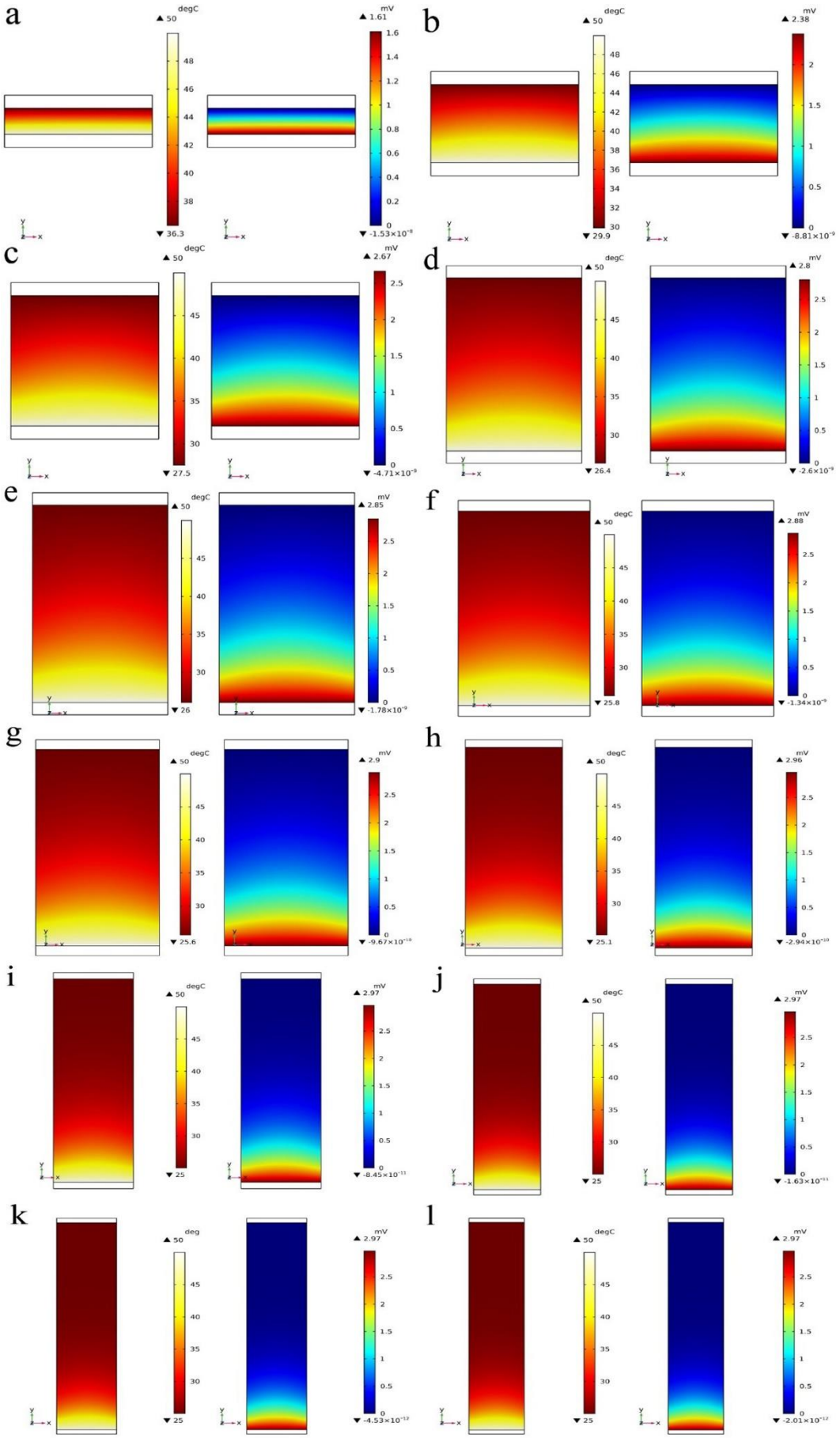
a
degC
▲ 50
48
46
44
42
40
38
▼ 36.3
mV
▲ 1.61
1.6
1.4
1.2
1
0.8
0.6
0.4
0.2
0
▼ -1.53×10⁻⁸
b
degC
▲ 50
48
46
44
42
40
38
36
34
32
▼ 29.9
mV
▲ 2.38
2
1.5
1
0.5
0
▼ -8.81×10⁻⁹
c
degC
▲ 50
45
40
35
30
▼ 27.5
mV
▲ 2.67
2.5
2
1.5
1
0.5
0
▼ -4.71×10⁻⁹
d
degC
▲ 50
45
40
35
30
▼ 26.4
mV
▲ 2.8
2.5
2
1.5
1
0.5
0
▼ -2.6×10⁻⁹
e
degC
▲ 50
45
40
35
30
▼ 26
mV
▲ 2.85
2.5
2
1.5
1
0.5
0
▼ -1.78×10⁻⁹
f
degC
▲ 50
45
40
35
30
▼ 25.8
mV
▲ 2.88
2.5
2
1.5
1
0.5
0
▼ -1.34×10⁻⁹
g
degC
▲ 50
45
40
35
30
▼ 25.6
mV
▲ 2.9
2.5
2
1.5
1
0.5
0
▼ -9.67×10⁻¹⁰
h
degC
▲ 50
45
40
35
30
▼ 25.1
mV
▲ 2.96
2.5
2
1.5
1
0.5
0
▼ -2.94×10⁻¹⁰
i
degC
▲ 50
45
40
35
30
▼ 25
mV
▲ 2.97
2.5
2
1.5
1
0.5
0
▼ -8.45×10⁻¹¹
j
degC
▲ 50
45
40
35
30
▼ 25
mV
▲ 2.97
2.5
2
1.5
1
0.5
0
▼ -1.63×10⁻¹¹
k
deg
▲ 50
45
40
35
30
▼ 25
mV
▲ 2.97
2.5
2
1.5
1
0.5
0
▼ -4.53×10⁻¹²
l
degC
▲ 50
45
40
35
30
▼ 25
mV
▲ 2.97
2.5
2
1.5
1
0.5
0
▼ -2.01×10⁻¹²

Figure S7. The numerically simulated temperature and potential fields of annealed $Ag_{2.3}Se$ films with different lengths. 1 mm (a), 3 mm (b), 5 mm (c), 7 mm (d), 8 mm (e), 9 mm (f), 10 mm (g), 13 mm (h), 16 mm (i), 20 mm (j), 23 mm (k) and 25 mm (l), related to Figure 9.

The temperature and potential fields of annealed $Ag_{2.3}Se$ films with different lengths (from 1 mm to 25 mm) are obtained via numerical simulation, and the results are listed in Figure S7. Notably, due to the changing aspect ratio, the width of simulated films looks different, but actually they are all 5 mm. It can be concluded from the temperature and potential fields that the temperature difference and open-circuit voltage (U_{oc}) increase with the ascending length of film and finally reach a steady state once the length exceeds 13 mm.

Table S1. The full width at half maximum (FWHM) values of (112) plane for all films before and after being annealed, related to Figure 1.

	FWHM of (112) plane (before annealing)	FWHM of (112) plane (after annealing)
$Ag_{1.9}Se$	0.164	0.098
$Ag_{2.0}Se$	0.198	0.144
$Ag_{2.1}Se$	0.209	0.148
$Ag_{2.2}Se$	0.192	0.106
$Ag_{2.3}Se$	0.196	0.116
$Ag_{2.4}Se$	0.191	0.097
$Ag_{2.5}Se$	0.208	0.136

As displayed in Table S1, for all annealed silver selenide films, the full width at half maximum (FWHM) values of dominant peak ((112) plane) are reduced, implying that the annealing treatment leads to the enhanced crystallinity of Ag_2Se phase.

Video S1. The video about bending cycles of annealed $Ag_{2.3}Se$ thermoelectric device, related to Figure 11.

It can be observed from this video that the bending radius is about 1 cm.